applied sciences

MDPI

Article

Quantification of the Area of the Highest Temperature in Equine Infrared Images

Małgorzata Maśko [1,*], Marta Borowska [2], Urszula Sikorska [1], Anna Ciesielska [1], Łukasz Zdrojkowski [3,*] and Małgorzata Domino [3,*]

1 Department of Animal Breeding, Institute of Animal Science, Warsaw University of Life Sciences (WULS–SGGW), 02-787 Warsaw, Poland; urszula_sikorska@sggw.edu.pl (U.S.); anna_ciesielska@sggw.edu.pl (A.C.)
2 Institute of Biomedical Engineering, Faculty of Mechanical Engineering, Białystok University of Technology, 15-351 Bialystok, Poland; m.borowska@pb.edu.pl
3 Department of Large Animal Diseases and Clinic, Institute of Veterinary Medicine, Warsaw University of Life Sciences (WULS–SGGW), 02-787 Warsaw, Poland
* Correspondence: malgorzata_masko@sggw.edu.pl (M.M.); lukasz_zdrojkowski@sggw.edu.pl (Ł.Z.); malgorzata_domino@sggw.edu.pl (M.D.)

Abstract: Infrared thermography is a valuable tool adapted for veterinary diagnostics with an increasing number of uses. However, proper image acquisition is hard, not only due to various factors affecting the image but also because informative image processing is a struggle. Thus, this study aims to quantify the area of maximum temperature (Area of Tmax) on the lateral surface of horses and foals to compare the Areas of Tmax between horses and foals and to compare two new approaches to the Area of Tmax quantification in horses. Infrared images were acquired with a thermographic camera from 12 horses and 12 foals in the same ambient condition. The backgrounds of the images were removed, and the images were then processed in Rainbow HC and a grayscale palette. Then, 10 images were created, showing the Areas of Tmax in gradually decreasing ranges. The evaluation of the Area of Tmax with two image processing methods showed higher maximum temperatures in foals, although the high-temperature values covered less of their total body area than in adult horses. The results indicate the struggles of foals with thermal homeostasis. The proposed methods—multi-colored annotated pixels on Rainbow HC and red-annotated pixels on grayscale—provide a common quality in the thermogram evaluation of foals and adult horses. Further research is essential to determine their diagnostic application.

Keywords: infrared thermography; foal; image processing; quantitative thermography

check for updates

Citation: Maśko, M.; Borowska, M.; Sikorska, U.; Ciesielska, A.; Zdrojkowski, Ł.; Domino, M. Quantification of the Area of the Highest Temperature in Equine Infrared Images. *Appl. Sci.* **2023**, *13*, 11006. https://doi.org/10.3390/app131911006

Academic Editor: Igor Pušnik

Received: 21 August 2023
Revised: 21 September 2023
Accepted: 24 September 2023
Published: 6 October 2023

1. Introduction

Similar to other objects, animal bodies radiate power that can be detected with specific tools. Thermographic cameras enable measurements of radiated energy, providing data about the surface temperature [1,2]. The amount of detected energy depends on many internal and external factors. Of the internal factors, the local increase in blood flow, increased tissue metabolism, and sweating can affect the infrared images, which offer the opportunity for diagnostic use. Of the external factors, ambient temperature, wind, humidity, and dirt play significant roles [1–3].

The basal metabolism of younger individuals is higher than that of adults, resulting in increased surface energy radiation [4]. This can be associated with the fast growth and development of muscles, but also with high motoric activity [5]. It was found that metabolism is associated with heart rate, making it a possible tool for metabolic rate evaluation [4]. In foals less than one month of age, cardiac output and respiration are not yet stabilized, which causes variations in both heart and respiratory rates. Also, heart rate measurement requires contact with the animal, which can induce a stress response and increase the measured values, meaning the result is then biased [4–6].

While there are helpful recommendations for nutrition in equines, they are not always precise as individuals vary [7]. This may result in malnutrition and maldevelopment of the growing foal. The main differences are found in housing systems and health conditions. Foals can be housed in low temperatures (open housing in colder climates), but they require an acclimatization period to maintain their health. But even then, their metabolic rate can be twice that of foals housed in a closed system, resulting in significantly higher nutritional demands, as maintenance demands exceed growth demands [4,6,8–11]. On the other hand, in sick foals, in which nutrient intake is decreased because of a disease, metabolic rates decrease, hampering proper growth [4]. Thus, proper evaluation of the nutritional demands of the individual foal can be challenging, as thermoregulation plays a major role in maintenance demands. The underestimation of demand increase will affect the growth process, especially at a younger age. Thus, expenses on foal homeothermy should be considered, but they are difficult to measure [7,8,10]. In grown horses, similar concerns arise, as housing, the training regime, and sport performance also cause variations in maintenance demands. Malnutrition in adults does not hamper growth and proper cartilage development; however, refeeding is still challenging, especially in older individuals [12,13].

Apart from increased metabolism, other features of young animals affect their thermoregulation. While insulation is provided by body fat and hair coat, fat tissue and effective hair coat develop with age, resulting in increased radiation [14,15]. This suggests that energy losses in foals are higher than in adults in similar ambient temperatures. Another factor having a big impact is the increased surface-area-to-weight ratio in young animals [8,16]. On the other hand, during training and in older horses, the emission of excessive heat is a big challenge. Ageing is also responsible for less effective cooling, and proper hydration, allowing for sweating, should be supplied for all [10,17].

Energy emission can be measured not only on animals but also on inanimate objects. Thus, radiation from nearby objects may affect the animal's measurements, especially in higher than ambient temperatures, which can occur with sun exposure. Air humidity, as well as the presence of dust, will also affect thermographic results, especially with an increasing distance from the examined objects [18]. Regardless of the aim, thermal images are also affected by the roughness of the examined surface, providing more precise results from smooth surfaces. Thus, in achieving credible and accurate thermographic images, experience, effort, and consequence are crucial [3,18,19].

The main advantage of infrared thermography (IRT) is that it is contactless for the patient, enabling its use even in wildlife [1,2,20,21]. In equine medicine, IRT can be used as a diagnostic tool to detect inflammatory areas, e.g., on the back [3,22] or limbs [3,23–25] and during pregnancy [26]. Measurements of surface temperatures can also be used to improve the welfare of leisure and sport horses [21,27,28], as well as enhance athletic performance by evaluating the adaptation of training methods to individuals [3,29,30]. Importantly, this diagnostic tool allows for multiple examinations as IRT is relatively easy to conduct and completely harmless for imaged animals [2,3,24].

Unfortunately, besides these advantages, there are limitations on the use of IRT in equine medicine. Achieving reliable results for both infrared image acquisition and image processing may prove difficult. The quality of hardware, user experience and knowledge, proper animal preparation, and environmental conditions affect image acquisition [2,21,24]. As there are multiple thermographic cameras on the market, it is not certain that all will provide similar quality results. Cheaper, more available cameras can have a larger margin of error and lower image resolution [24]. Human-dependent factors can also play a role in imaging domestic animals; for the highest quality infrared images, animals should be properly prepared by cleaning, grooming, and brushing [4,24,31,32]. The major challenge of image processing is to apply regions of interest (ROIs) on infrared images, which is crucial for numerical data extraction (ROI quantification) and comparisons between regions on both sides of an animal [1,2,20,33,34]. Most commercial software allows for an application of ROIs, which are circular, rectangular, or linear; however, undoubtedly, they are not adequate for all body regions or groups of muscles, as a horse's surface demonstrates a complex, irregular shape. Recently developed software enables the quantification of irregular shapes. Yet, still, infrared image segmentation [35] and the development of a new quantification method [21,22,33,34,36] have been the object of recent research to achieve a particular aim, which is extracting more data from IRT to human [35] and veterinary [21,22,33,34,36] diagnostics than that currently available [3,21,24,26,31].

Several studies regarding veterinary medicine applications have focused on measurements of the area with the highest temperature (Area of Tmax) [26,31]. Such an approach may enable the evaluation of a horse's health and condition in a more comprehensive manner. The activation of brown adipose tissue, important in thermogenesis, can be informative for wild equids housed in captivity, free-range horses, or foals, in which many processes are not fully developed yet. General thermogenesis efficiency can be assessed using infrared images [1,28,37,38]. It is important to assess whether peripheral body areas are set to emit more heat, or to decrease emissions by the constriction of peripheral vessels, as both processes require energy and can decrease animal welfare [27,28]. The Area of Tmax can be also used in assessing changes in thermogenesis associated with age, development of the process in foals, but also gradual decreases in thermoregulation effectiveness in older horses [10,17,39–41]. The Area of Tmax was proposed as a feature helpful in pregnancy diagnosis in late gestation; however, this was only applicable in a range of 3 °C [2]. As previous results were promising, an adaptation of and improvement in the Area of Tmax-dependent method are proposed here in order to improve its usage in equine medicine. Especially regarding the evaluation of individual nutritional requirements, there is a need to develop an easy and repeatable method for a thermoregulation expenses assessment. Thus, the goal is to facilitate thermography to increase the applicability, repeatability, and specificity of the Area of Tmax method, as well as thermography itself. We are hoping that the proposed method of Area of Tmax utilization will facilitate the wider use of thermography, including an improvement in the accuracy of thermograms, despite the multitude external factors affecting it [18,19]. Especially given that, in some cases, it is not possible to overcome the limitations of infrared image acquisition to reduce their influence, although image processing can be improved. This study aims (a) to detect and quantify the Area of Tmax across the lateral surface of horses and foals, respectively; (b) to compare the Areas of Tmax between horses and foals; (c) and to compare two methods of the Area of Tmax quantification.

2. Materials and Methods

2.1. Animals

Infrared images of the lateral side of 12 mature horses and 12 foals were analyzed. For the herd of 90 Konik Polski horses, 12 mature horses (mean age 5.67 ± 1.44 years; within 8 mares and 4 stallions) and 12 foals (mean age 6.06 ± 0.27 months; within 7 mares and 5 stallions) were imaged. All animals were housed in an all-day open stable in a Polish state horse farm called Dobrzyniewo where the conservation breeding of Konik Polski horses is carried out. All animals were housed under the same management protocol, including feeding twice a day (dose of hay fit to each horse to maintain optimal condition), constant access to fresh water and a salt lick, and daily access to a pasture (a large grassy area for no less than 12 h per day).

2.2. Infrared Imaging

All animals were imaged following international guidelines for conducting thermographic imaging in equine clinical practice [3]. All animals were imaged on the same day in the morning when the ambient temperature was 20.1 °C and relative humidity was 50.6%. All animals were imaged indoors in a stable, in a closed space, protected from wind and sun radiation, to minimize the influence of external environmental conditions. On the day of imaging, the horses were locked in the stable from the morning and went out to the pasture only after the imaging had been conducted, which was before noon. The researcher entered the stable along with a staff member familiar with animals to decrease the influence of stress. All animals were brushed to remove dirt and mud 30 min before imaging.

Images were taken on the right or left side of the animal's body using a non-contact thermographic camera (FLIR Therma CAM E60, FLIR Systems, Brazil; emissivity (e) 0.99) [2,24,30,31]. The camera was positioned to cover the entire lateral surface of the animal—at approximately 2 m from the animal's body surface with the center of the field of view orientated to the intersection of two lines—with a horizontal line drawn through the shoulder joint and a vertical line drawn behind the last rib. All images were obtained by the same researcher (MM).

2.3. Images Processing

Raw images (Figure 1A) were initially processed using the commercial infrared camera software (FLIR Tools, FLIR Systems Brasil, Brazil) by setting the Rainbow HC palette and temperature range between 15.0 and 50.0 °C (Figure 1B). The rectangle drawing tool (Bx) was used to determine the anatomical regions with the highest/maximal temperatures (Tmax) on the animal's body surface (Figure 1C). A Tmax value was obtained for each animal, which was used to return the subsequent Area of Tmax images in the following steps. Since in the Rainbow HC palette most of the background below the limit temperature (set to 15 °C) was masked with black (hexadecimal color code value (HEX) color #000000), the rest of the background was manually masked using HEX color #000000 in the paint net. v.4.3.2 software (Figure 1D) so that the whole non-#000000 pixels area represented the animals' surfaces. Thus, the additional image segmentation was redundant, and automatic segmentation was applied in the next step. FLIR Tools enables the delineation of irregular shapes; however, it was not used for the Area of Tmax application.

Each image was saved as a BMP file, 1111 pixels wide x 817 pixels high. In the Rainbow HC palette, 10 images were obtained for each animal by changing the setting of the lower temperature range from Tmax-1 °C to Tmax-10 °C (Figure 1E). Then, a subsequent 10 images in the Gray palette were obtained for each animal, using the alarm tool above a certain temperature, by changing the setting of the alarm limit range from Tmax-1 °C to Tmax-10 °C in the temperature range between Tmax-10 °C and 50.0 °C. The temperature above the set limit was annotated in red (Figure 1F). The masking procedure was repeated for each image. In this way, images of the animals were obtained, and these were then completely subjected to further analysis without the need for image segmentation.

The lower temperature range in the Rainbow HC palette images and alarm limit in the Grayscale palette images was changed in order to obtain images with colored areas (non-#000000 pixels), multi-colored-annotated pixels (Figure 2), and red-annotated pixels (Figure 3), respectively. For the Areas of Tmax, multi-colored-annotated pixels from the Rainbow HC palette images and red-annotated pixels from Grayscale palette palette images were used in the procedure for counting the annotated pixels in infrared images.

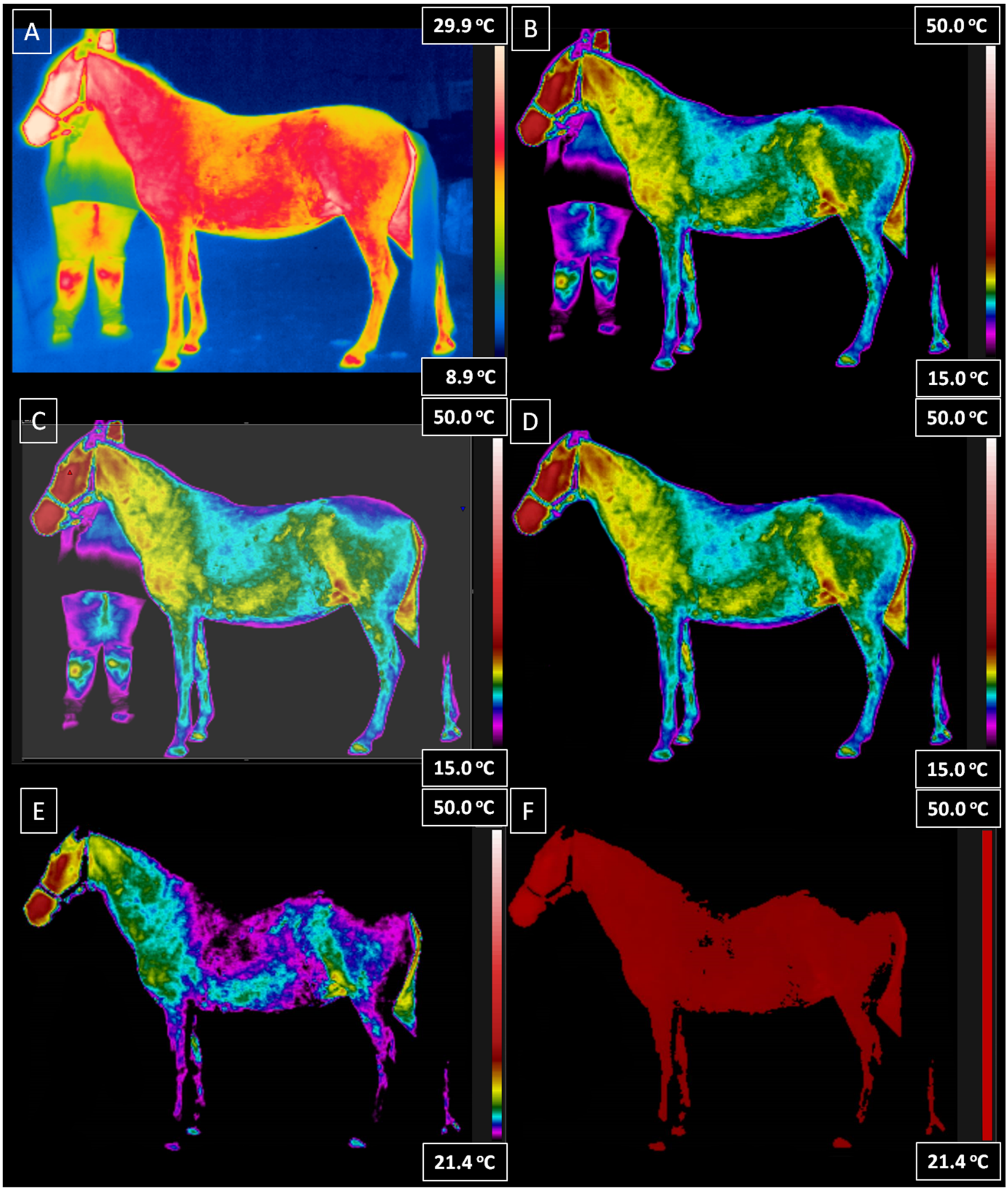

Figure 1. Infrared images of the lateral surface of the horse. (**A**) Raw image; (**B**) basic image in Rainbow HC palette with temperature range set between 15.0 and 50.0 °C; (**C**) image in Rainbow HC palette with marked the highest/maximal temperatures (Tmax) in the horse's eye area; (**D**) image in Rainbow HC palette with background masked; (**E**) image in Rainbow HC palette with temperature range set between Tmax-10 °C and 50.0 °C; (**F**) image in Gray palette with temperature range set between Tmax-10 °C and 50.0 °C and alarm tool set on Tmax-10 °C limit.

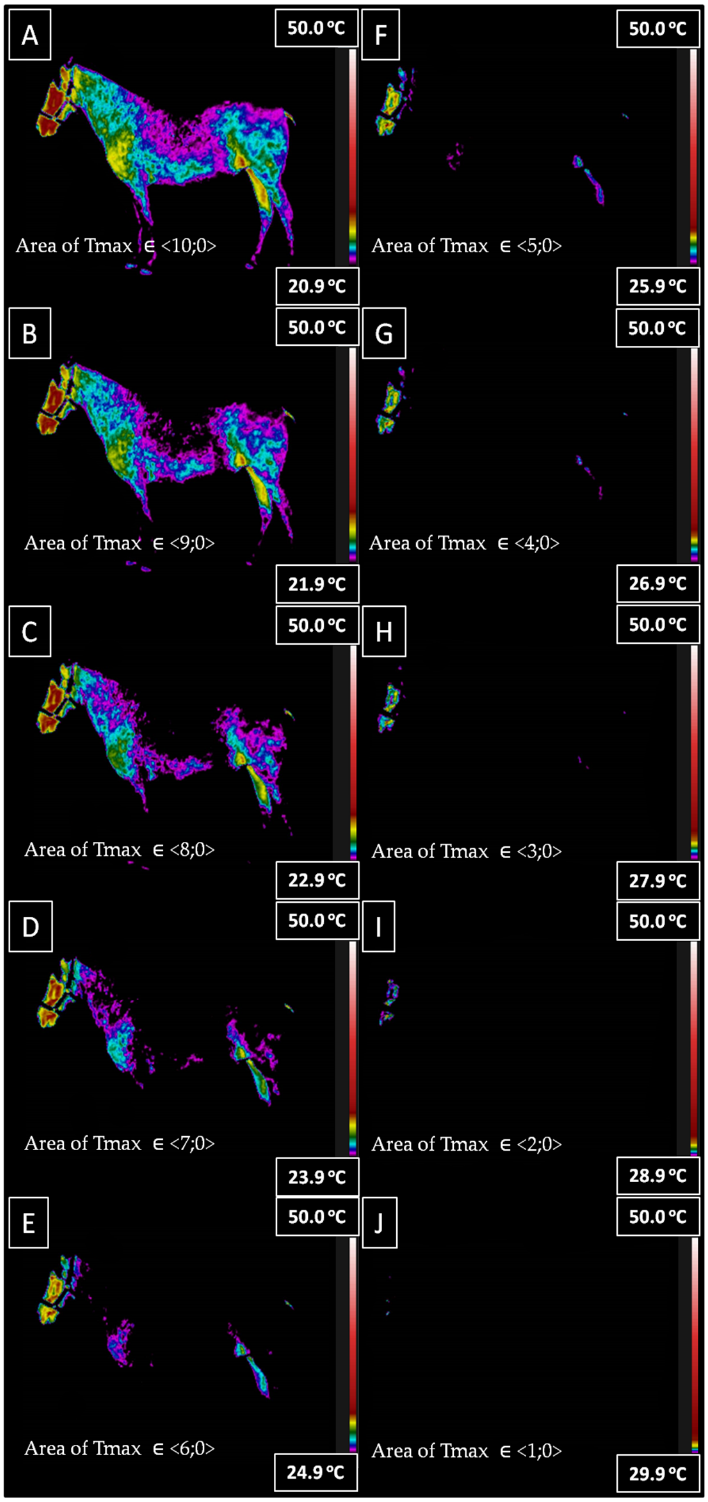

Figure 2. Processed infrared images of the lateral surface of the horse. The area of the highest/maximal temperatures (Tmax) is marked as the multi-colored-annotated area on the Rainbow HC palette images. (**A**) The ranges for Tmax-10 °C; (**B**) Tmax-9 °C; (**C**) Tmax-8 °C; (**D**) Tmax-7 °C; (**E**) Tmax-6 °C; (**F**) Tmax-5 °C; (**G**) Tmax-4 °C; (**H**) Tmax-3 °C; (**I**) Tmax-2 °C; and (**J**) Tmax-1 °C are marked on the respective images.

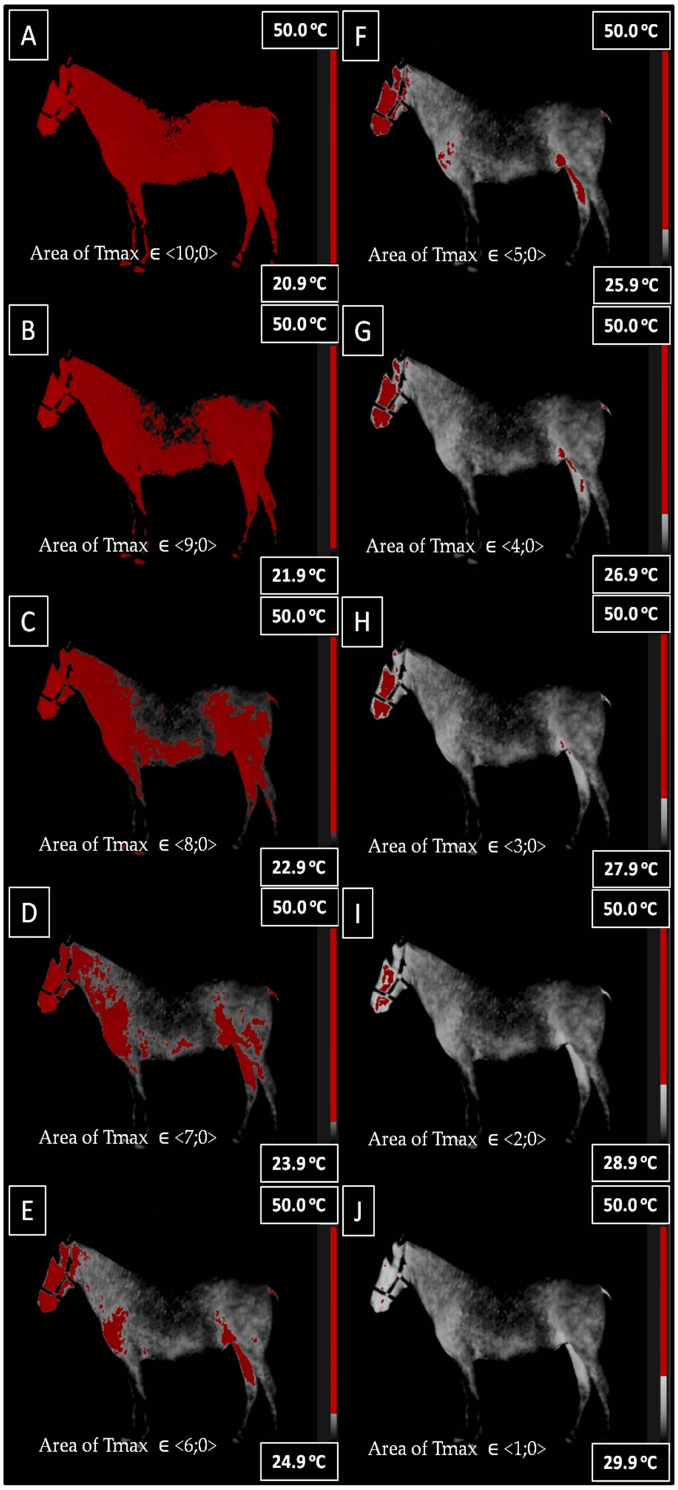

Figure 3. Processed infrared images of the lateral surface of the horse. The area of the highest/maximal temperatures (Tmax) is marked as the red-annotated area on the Grayscale palette images. (**A**) The ranges for Tmax-10 °C; (**B**) Tmax-9 °C; (**C**) Tmax-8 °C; (**D**) Tmax-7 °C; (**E**) Tmax-6 °C; (**F**) Tmax-5 °C; (**G**) Tmax-4 °C; (**H**) Tmax-3 °C; (**I**) Tmax-2 °C; and (**J**) Tmax-1 °C are marked on the respective images.

Color analysis was performed on infrared images using the color histogram method from the extcolors package in Python (https://pypi.org/project/extcolors/, accessed on

24 July 2023). This technique involves grouping colors based on visual similarity calculated from a CIE76 Formula (1):

$$\Delta E^* = \sqrt{}((\Delta L^*) + (\Delta a^*) + (\Delta b^*)) \quad (1)$$

In this formula, the CIELAB color space was used. The CIELAB color space is referred to as L*a*b*, where L* is the perceptual lightness, whereas both a* and b* are four unique colors of vision (red, green, blue, and yellow) represented by the chrome plane. In this approach, two colors in CIELAB color space are represented (L_1*, a_1*, b_1*) and (L_2*, a_2*, b_2*), where:

$$\Delta L^* = (L\_2^* - L\_1^*)$$

$$\Delta a^* = (a\_2^* - a\_1^*)$$

$$\Delta b^* = (b\_2^* - b\_1^*)$$

Moreover, $\Delta E^* \approx 2.3$ corresponds to a just noticeable difference [41].

The method resulted in a text representing a list (from the most used) of ascending colors in the image and the number of corresponding pixels. The colors were defined in RGB format. The conversion of the RGB codes into HEX color codes was then carried out using the rgb2hex library (https://colormap.readthedocs.io/en/latest/, accessed on 24 July 2023). Automatic segmentation was applied to encompass the entire surface of the animal in the ROI. The numerical results were presented as the occurrence (number of pixels) of a given color in the image referring to the ROI. Visualization of the results is presented via a pie chart.

The total occurrence of multi-colored-annotated pixels (Total pixels) was counted on the basic image in the Rainbow HC palette. This value was used for each image to calculate the percentage of multi-colored-annotated pixels (Color pixels) occurrence and the percentage of red-annotated pixels (Red pixels) occurrence.

2.4. Statistical Analyses

Univariate marginal distributions of demographic data (age) and thermal data (Total pixels, Tmax, % of Color pixels, % of Red pixels) were independently tested for normality using a Shapiro–Wilk test for each image. The distribution of age, Total pixels, and Tmax were normal in the horse and foal groups, whereas the distribution of the parts of the % of Color pixels and % of Red pixels was not normal in at least one group. Therefore, mean + SD was used to present age, Total pixels, and Tmax, whereas the median ± quartiles was used to present the % of Color pixels and % of Red pixels. The comparison of data pairs showing normal distribution was assessed using an unpaired t-test with Welch's correction, whereas those not showing normal distribution were assessed using the Mann–Whitney test. The significance level was set as $p < 0.05$. The t-value and df were displayed on each plot.

Linear regression was used to compare Total pixels, the % of Color pixels, and the % of Red pixels with respect to the consecutive Areas of Tmax. Two regression equations and r-squares were presented on each plot. All the slopes were significantly non-zero ($p < 0.0001$). Initially, the slopes in total pixels for the horses equation and total pixels for the foals equation were compared. Secondly, the slopes in the % of Color pixels for the horses equation and % of Red pixels for the horses equation were compared. Finally, the slopes in the % of Color pixels for the foals equation and % of Red pixels for the foals equation were compared. When differences between the slopes were not significant ($p > 0.05$), a single slope was calculated for both datasets. Then, the intercepts were compared. When differences between the intercepts were not significant ($p > 0.05$), a single intercept was calculated for both datasets. All statistical analyses were performed using GraphPad Prism6 software (GraphPad Software Inc., Boston, MA, United States).

3. Results

In the infrared images representing the entire body surface of the imaged animals, the horse group exhibited a pixel count ranging from 203,638 to 320,695 pixels, while the foal group ranged from 205,421 to 322,355 pixels. In the horse group, these pixels displayed from 15 to 21 colors, while in the foal group, 18 to 22 colors were displayed (Figure 4).

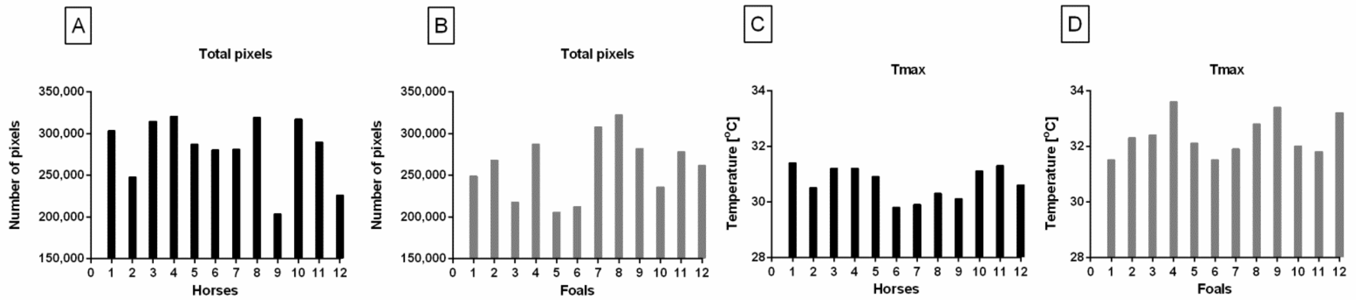

Figure 4. Histograms of (**A**,**B**) the total occurrence of multi-colored-annotated pixels (Total pixels) and (**C**,**D**) the highest/maximal temperatures (Tmax) determined for the following: (**A**,**C**) horses and (**B**,**D**) foals.

The main colors detected in the infrared images are presented in Figures 5 and 6. In the horse group, pixels in shades of dark green (Figure 5A–D,F–H) and light green (Figure 5E,I–L) were most frequently detected. Pixels in shades of light blue (Figure 5A,B,E) and dark blue (Figure 5F,G) were less common. In the foal group, pixels in shades of green, both dark and light, were most prevalent (Figure 6A,B,E,F,I–L), whereas pixels in shades of blue were detected less frequently (Figure 6C,D). In both groups, pixels in shades of red, purple, and orange accounted for a smaller percentage. However, there was no significant difference in Total pixels between the horse and foal groups ($p = 0.17$; Figure 7A).

On the other hand, Tmax was higher in the foal group than the horse group ($p < 0.0001$; Figure 7B). Tmax ranged from 29.8 °C to 31.4 °C in the horse group, whereas in the foal group, Tmax ranged from 31.5 °C to 33.6 °C. Interestingly, the highest temperature values were observed in horses in the eye, nostrils, and temporal regions, whereas in foals, these were only in the eye region (Table 1).

Table 1. The highest/maximal temperatures (Tmax) determined for the following anatomical regions of the horses' (n = 12) and foals' (n = 12) body surfaces.

Horses	**1**	**2**	**3**	**4**	**5**	**6**	**7**	**8**	**9**	**10**	**11**	**12**
Tmax region	31.4 °C eye	30.5 °C nostrils	31.2 °C eye	31.2 °C temporal	30.9 °C nostrils	29.8 °C eye	29.9 °C eye	30.3 °C nostrils	30.1 °C eye	31.1 °C eye	31.3 °C eye	30.6 °C eye
Foals	**1**	**2**	**3**	**4**	**5**	**6**	**7**	**8**	**9**	**10**	**11**	**12**
Tmax region	31.5 °C eye	32.2 °C eye	32.4 °C eye	33.6 °C eye	32.1 °C eye	31.5 °C eye	31.9 °C eye	32.8 °C eye	33.4 °C eye	32.0 °C eye	31.8 °C eye	33.2 °C eye

The similarities between the Total pixels detected in the horse and foal groups throughout ten Areas of Tmax were tested using a linear regression model. The slope of the linear regression equations for Total pixels in the horse group compared to the slopes of Total pixels in the foal group was significantly different ($p < 0.0001$); thus, no single slope was calculated (Figure 5C). Therefore, no evidence of similarity in the distribution of Total pixels between these two groups can be noted.

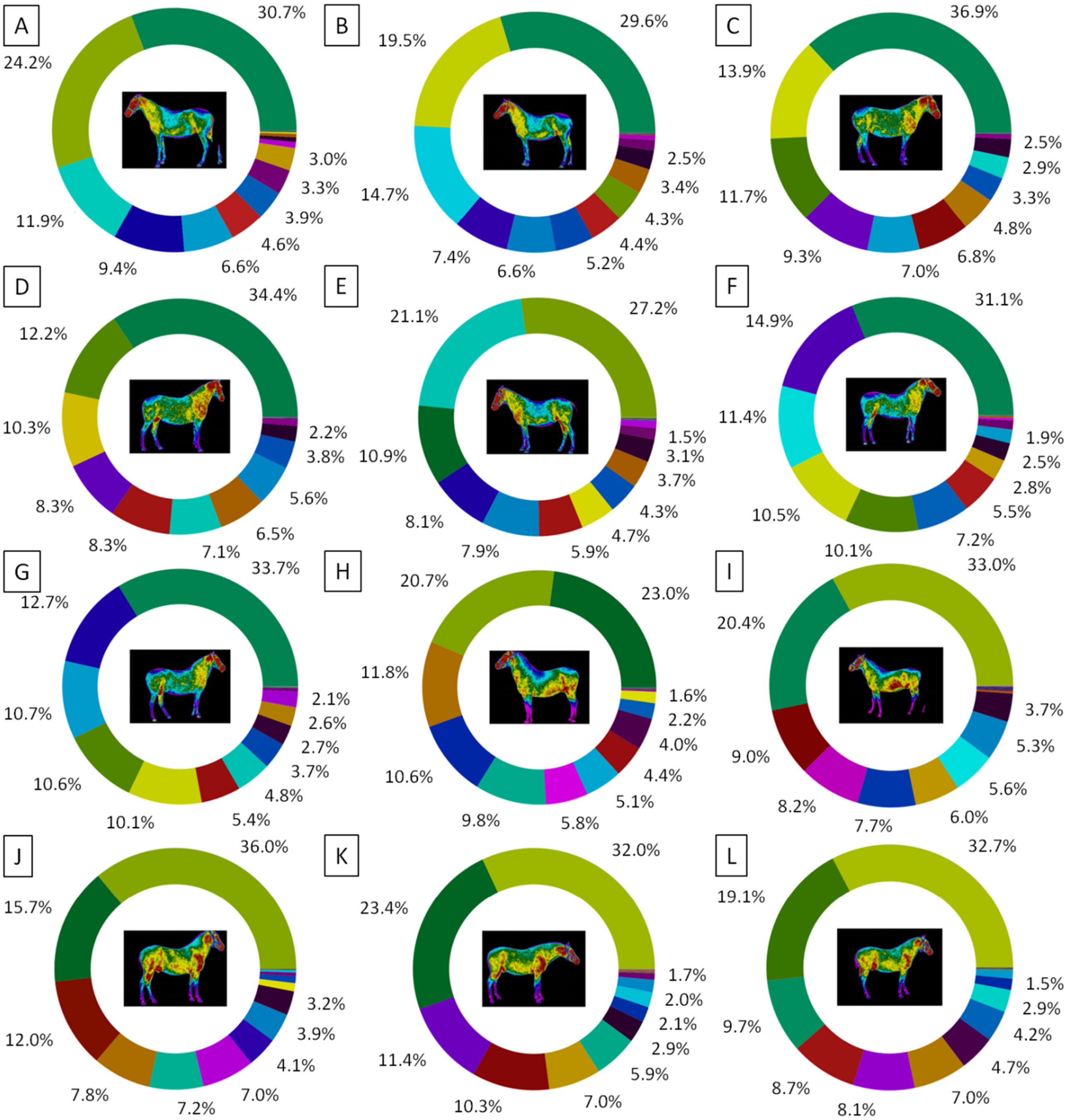

Figure 5. Percentage of pixels belonging to individual HEX colors detected on the horses' body surface. Subsequent horses were considered separately as individuals 1–12 (**A–L**). Percentage of pixels < 1.5% is not displayed.

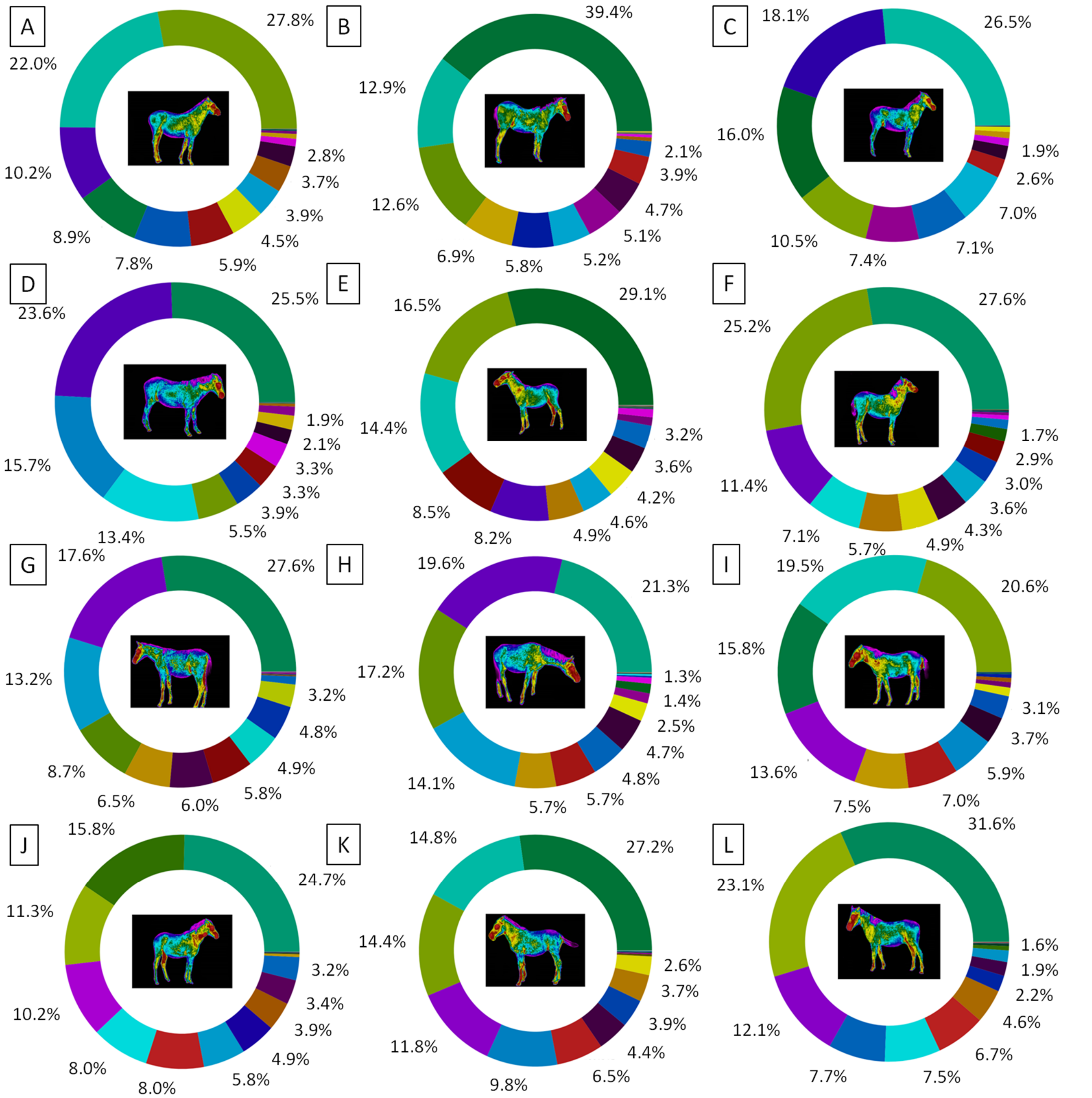

Figure 6. The percentage of pixels belonging to individual HEX colors detected on the foals' body surface. Subsequent foals were considered separately as individuals 1–12 (**A**–**L**). Percentage of pixels < 1.5% is not displayed.

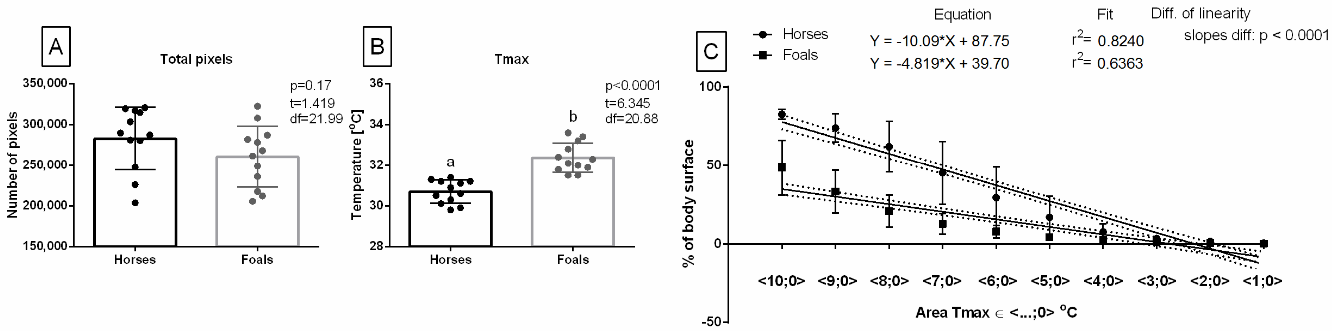

Figure 7. (**A**) The total occurrence of multi-colored-annotated pixels (Total pixels) and (**B**) the highest/maximal temperatures (Tmax) compared between horse and foal groups. Data in bar graphs were represented as the mean + SD. Additionally, values for subsequent individuals were marked with dots. Lowercase letters indicate differences between the horse and foal groups for $p < 0.05$. (**C**) Comparison of Total pixels detected in the horse and foal groups throughout ten Areas of Tmax ranging from Tmax−10 °C <10, 0> to Tmax−1 °C <1, 0>. Similarity was tested using linear regressions and considered significant for $p < 0.05$. The t-value and df are displayed on the plots (**A**,**B**).

Then, the % of Color pixels was compared between the horse and foal groups for each Area of the Tmax separately. The % of Color pixels was found to be higher in the horse group than in the foal group in the following ranges: Tmax-10 °C ($p < 0.0001$; Figure 8A), Tmax-9 °C ($p < 0.0001$; Figure 8B), Tmax-8 °C ($p < 0.0001$; Figure 8C), Tmax-7 °C ($p = 0.0001$; Figure 8D), Tmax-6 °C ($p = 0.003$; Figure 8E), Tmax-5 °C ($p = 0.0002$; Figure 8F), Tmax-4 °C ($p < 0.0001$; Figure 8G), Tmax-3 °C ($p < 0.0001$; Figure 8H), Tmax-2 °C ($p = 0.0003$; Figure 8I), and Tmax-1 °C ($p = 0.03$; Figure 8J).

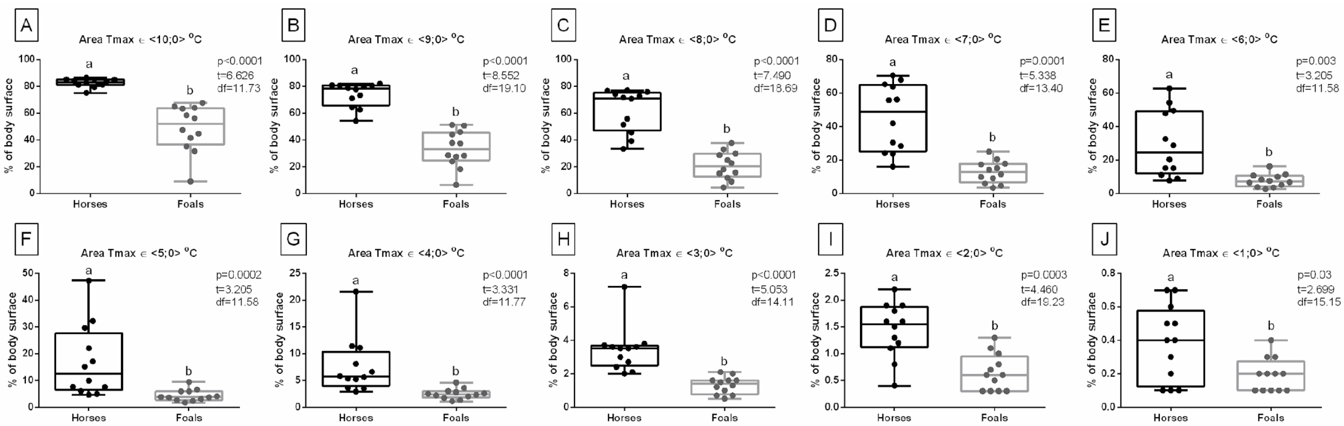

Figure 8. The percentage of multi-colored-annotated pixels (Color pixels) occurrence in the Areas of the highest/maximal temperatures (Tmax) ranged for (**A**) Tmax-10 °C; (**B**) Tmax-9 °C; (**C**) Tmax-8 °C; (**D**) Tmax-7 °C; (**E**) Tmax-6 °C; (**F**) Tmax-5 °C; (**G**) Tmax-4 °C; (**H**) Tmax-3 °C; (**I**) Tmax-2 °C; and (**J**) Tmax-1 °C. Data in box plots were represented by the lower quartile, median, and upper quartile, whereas whiskers represent minimum and maximum values. Additionally, values for subsequent individuals were marked with dots. Lowercase letters indicate differences between horse and foal groups for $p < 0.05$. The t-value and df are displayed on each plot.

Similarly, the % of Red pixels was compared between the horse and foal groups for each Area of the Tmax separately. The % of Red pixels was higher in the horse group than in the foal group in the following ranges: Tmax-10 °C ($p < 0.0001$; Figure 9A), Tmax-9 °C ($p < 0.0001$; Figure 9B), Tmax-8 °C ($p < 0.0001$; Figure 9C), Tmax-7 °C ($p < 0.0001$; Figure 9D), Tmax-6 °C ($p = 0.002$; Figure 9E), Tmax-5 °C ($p = 0.0008$; Figure 9F), Tmax-4 °C ($p < 0.0001$; Figure 9G), Tmax-3 °C ($p < 0.0001$; Figure 9H), Tmax-2 °C ($p = 0.0004$; Figure 9I), and Tmax-1 °C ($p = 0.008$; Figure 9J).

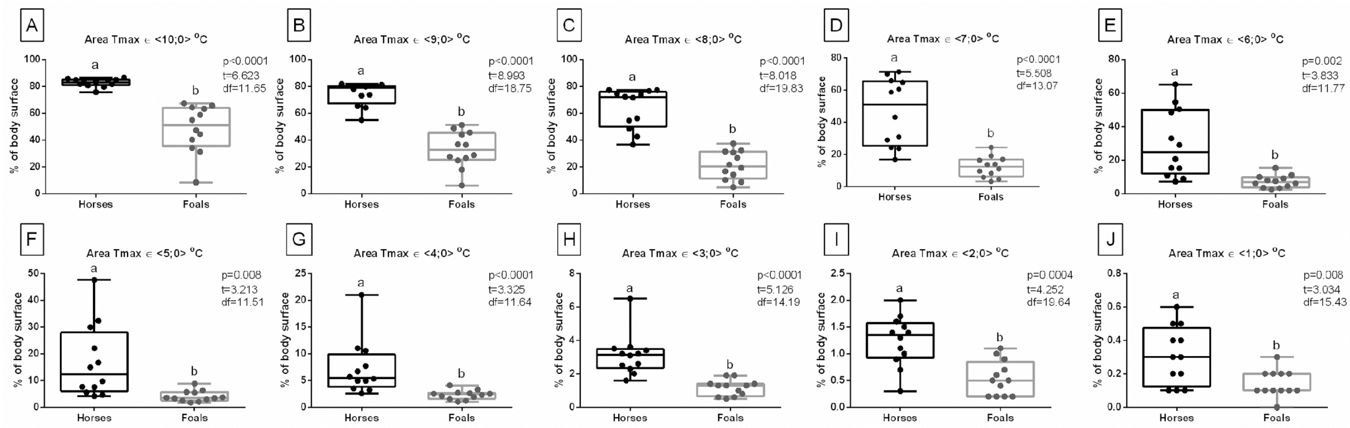

Figure 9. The percentage of red-annotated pixels (Red pixels) occurrence in the Areas of the highest/maximal temperatures (Tmax) ranged for (**A**) Tmax-10 °C; (**B**) Tmax-9 °C; (**C**) Tmax-8 °C; (**D**) Tmax-7 °C; (**E**) Tmax-6 °C; (**F**) Tmax-5 °C; (**G**) Tmax-4 °C (**H**) Tmax-3 °C; (**I**) Tmax-2 °C; and (**J**) Tmax-1 °C. Data in box plots were represented by the lower quartile, median, and upper quartile, whereas whiskers represent minimum and maximum values. Additionally, values for subsequent individuals were marked with dots. Lowercase letters indicate differences between horse and foal groups for $p < 0.05$. The t-value and df were displayed on each plot.

Finally, the similarities between the % of Color pixels and % of Red pixels throughout the ten Areas of Tmax were tested using the linear regression model for the horse group (Figure 10A) and the foal group (Figure 10B) separately.

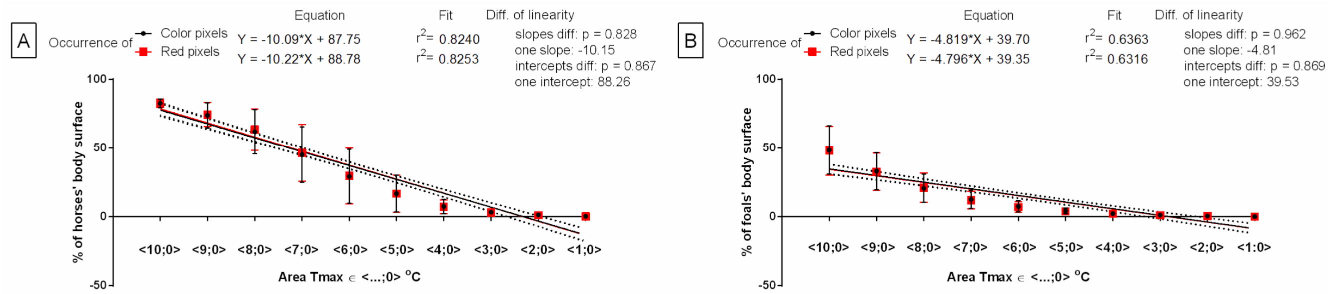

Figure 10. Comparison of the percentage of multi-colored-annotated pixels (Color pixels) and percentage of red-annotated pixels (Red pixels) occurrence throughout ten Areas of the highest/maximal temperatures (Tmax) ranged for Tmax−10 °C <10, 0> to Tmax−1 °C <1, 0>. The comparison was made separately for (**A**) the horse group and (**B**) the foal group. Similarity was tested using linear regressions and considered significant for $p < 0.05$. If the difference between slopes was not significant ($p > 0.05$), a single slope was calculated. If the difference between intercepts was not significant ($p > 0.05$), a single intercept was calculated.

In the horse group, the slope of the linear regression equation for the % of Color pixels compared to the slopes of the equation for the % of Red pixels was not significantly different ($p = 0.828$), and a single slope was calculated (one slope = −10.15). Moreover, the intercepts for both equations were not significantly different ($p = 0.867$), and a single intercept was calculated (one intercept = 88.26) (Figure 10A). Similarly, in the foal group, the slope of the linear regression equation for the % of Color pixels compared to the slopes of the equation for the % of Red pixels was not significantly different ($p = 0.962$), and a single slope was calculated (one slope = −4.81). The intercepts for both equations were not significantly different ($p = 0.869$), and a single intercept was calculated (one intercept = 39.53) (Figure 10B). Therefore, high similarity between these two approaches to the pixel-counting protocols can be confirmed in both groups.

4. Discussion

The total number of multi-colored-annotated pixels did not differ between foals and adult horses; thus, further analyses regarding comparisons of transformed infrared images are justified. Although these are still metabolically different groups, measured differences would provide new insights into the mechanisms of transition into developed homeothermy in adults. We have found higher surface temperatures in foals than in adult horses, confirming higher heat energy radiation associated with their higher metabolism related to growth and development, as well as smaller insulation [15,41–43]. Smaller insulation also contributed to detection areas with the highest temperature values both in adults and foals [3,21,30]. Although data regarding surface temperature in foals are scarce, it is well known that other temperature measurements confirm a higher physiological temperature in foals than in adult horses [10,40,41]. Therefore, to the best of our knowledge, this is the first report comparing IRT features, both conventional Tmax and novel Area Tmax, between adult and young horses.

While a different image processing method was used, most of the limitations primarily concern the complexity of acquiring reliable infrared images [3,18,19]. Variations in the background radiation were minimized by acquiring images in a closed stable with no surfaces exposed to sunlight. This ensured that the temperatures of the animals' surfaces were significantly higher than the background. The distance from the object not only affects the measured temperature values but also the homogeneity of the image. Along with distance, the influence of global radiation and atmospheric composition increases, especially within the first 20 m from the object [18,19]. In this study, the average distance was 2 m, reducing signal disruption and maintaining image homogeneity. For foals, we focused on the acquisition of a similar number of pixels from each individual, following recommendations [3,18,19]. Coat thickness, which varies between foals and adults, affects the amount of radiated energy [2,31]. We examined only the Polish Konik breed, which is quite uniform regarding hair coat, in an effort to minimize the influence of this variable. On the other hand, it is also crucial to assess the potential influence of stress and exertion immediately before image acquisition [2,24,29,30]. An altered physiological state in the animal can obscure the effects of other variables and may not provide data about the resting metabolic maintenance rate; thus, we paid close attention to minimizing through adjustment to the daily routine.

Jodkowska et al. (2011) have found Tmax in the horse body at rest to be 31.0 ± 1.7 °C, which corresponded with our Tmax range in the examined adults [44]. Their value was measured in the head region, although the authors did not separate it into smaller areas. In the available literature, there is a lack of data regarding Tmax in the foal body at rest; however, the head region in foals is also suspected of being the warmest due to its high blood supply, relatively low insulation provided by the hair coat, and fat tissue [3,30]. Similarly to the available data, we found the highest temperature in adults to be in the regions of the eye and nostrils; however, we included the temporal region as well [2]. In contrast to adult horses, we have found the highest temperature in foals to be only in the eye region. While this region is considered to be a thermographic marker of stress, we did not observe any stress signs in the animals during image acquisition. They exhibited normal behavior because the images were taken of untied, freely moving animals without physical contact. Moreover, the temperature of the foals' limbs differs less from the rest of the body compared to adults. This may show that foals are less capable of saving heat in this region due to conduction between arteries and veins [45].

The lower coverage of the Area of Tmax for all subtracted values indicates a less uniform temperature pattern, reflecting the foals' struggle to reduce heat emissions and maintain their body temperature. This leads to the faster cooling of peripheral body parts. Conversely, the higher slope observed in adult horses suggests that only a minimal part of the body is vulnerable to heat loss, while the rest of the central parts of the body remain steadily warm. This finding aligns with other thermographic studies that have shown higher temperatures in the trunk, neck, and head compared to the limbs [3,28,31,44].

The results show that in the context of metabolism, thermogenesis, and thermal homeostasis, foals should be handled separately from adult horses. Therefore, further research is needed to determine the physiological patterns of surface temperature and Area of Tmax for foals of different ages, serving as benchmarks for thermographic assessments of foal health and welfare within specific age groups. Otherwise, by treating a foal as an adult horse, we run the risk that an increased Tmax or a decreased Area if Tmax will be misinterpreted in the diagnostic procedure. Healthy foals, when provided with an adequate nutrient supply, should be capable of maintaining thermal homeostasis, yet special attention should be directed towards neonates, premature, weaker, or sick individuals, especially in terms of their housing conditions [15,40,41,43,46]. Furthermore, considering housing and nutritional adaptation, foals require careful treatment, as developing thermoregulation makes them more vulnerable to heat loss, leading to higher metabolic maintenance expenses [4,8,15,40]. We hope that image processing using the Area of Tmax can help to better understand the differences between foal and adult horse management and thermoregulation maturation in growing horses. Exploring these differences can contribute to the precise application of appropriate nutrition for young animals, enabling their healthy growth, which in turn allows them to fulfill their performance potential and improves their overall welfare [7,8,16,32].

Interestingly, both pixel annotation methods on both color scales have shown similar values in the evaluation of infrared images. Since no significant differences were found in either foals or adult horses between these two methods, it may be stated that they may be equally useful for the Area of Tmax assessment. In the multi-colored-annotated pixels method, colored pixels are displayed separately, with most of the background being automatically masked in black at the level of commercial thermographic software. On the other hand, in the red-annotated pixels method, pixels in shades of red are displayed against a background of pixels in shades of gray, representing the shape of the horse's body surface with a temperature below the set Tmax. This representation of infrared images simplifies the manual masking of the background using additional commercial graphics software, which makes the additional image segmentation redundant. This advancement should be considered a significant convenience, especially when compared to the laborious manual segmentation of infrared images using ROIs in commercial thermographic software. While the main direction of advanced infrared image analysis focuses on ROIs analyses [3,21,26,34,47,48], we provide a new tool for entire animal body evaluation. However, since we have only demonstrated its application in the characterization of infrared images in healthy horses, further research using the provided methods is necessary to develop their diagnostic use.

5. Conclusions

The evaluation of the Area of Tmax using two image processing methods has revealed the struggles of foals with a reduction in heat losses. Foals encounter more problems in maintaining thermal homeostasis compared to adult horses, and their thermal pattern is more variable. The presented methods provide a tool to evaluate energy losses in both foals and adult horses. Both methods, multi-colored-annotated pixels on the Rainbow HC palette and red-annotated pixels on the greyscale palette, offer consistent quality in the evaluation of thermograms for both groups: foals and adult horses. They can be considered as alternatives to simple and complex ROI quantification methods. Further research employing these methods on different breeds and growing horses will be essential to review their diagnostic applications in assessing nutritional demands.

Author Contributions: Conceptualization, M.M., M.B. and M.D.; methodology, M.M., M.B. and M.D.; software, M.B.; validation, M.M.; formal analysis, M.M., M.B., Ł.Z. and M.D.; investigation, M.M., U.S., A.C., Ł.Z. and M.D.; resources, M.M.; data curation, M.M.; writing—original draft preparation, M.M., M.B., Ł.Z. and M.D.; writing—review and editing, M.M., M.B., U.S., A.C. and M.D.; visualization, M.B. and M.D.; supervision, M.D.; project administration, M.M.; funding acquisition, M.M. and M.B. All authors have read and agreed to the published version of the manuscript.

Funding: The study was performed as part of the projects WI/WM-IIB/2/2021 and was partially financed with funds from the Polish Ministry of Science and Higher Education.

Institutional Review Board Statement: The study was conducted according to the guidelines of the Declaration of Helsinki and approved by the II Local Ethical Committee on Animal Testing in Warsaw on behalf of the National Ethical Committees on Animal Testing (protocol code WAW2/034/2018 and date of approval 27 April 2018).

Informed Consent Statement: Not applicable.

Data Availability Statement: The data presented in this study are available on request from the corresponding author.

Conflicts of Interest: The authors declare no conflict of interest.

References

1. Tattersall, G.J. Infrared Thermography: A Non-Invasive Window into Thermal Physiology. *Comp. Biochem. Physiol. Part A Mol. Integr. Physiol.* **2016**, *202*, 78–98. [CrossRef] [PubMed]
2. Soroko, M.; Davies Morel, M.C. *Equine Thermography in Practice*; CABI: Wallingford, UK, 2016.
3. Soroko, M.; Howell, K. Infrared Thermography: Current Applications in Equine Medicine. *J. Equine Vet. Sci.* **2018**, *60*, 90–96. [CrossRef]
4. Ousey, J.C.; McArthur, A.J.; Murgatroyd, P.R.; Stewart, J.H.; Rossdale, P.D. Thermoregulation and Total Body Insulation in the Neonatal Foal. *J. Therm. Biol.* **1992**, *17*, 1–10. [CrossRef]
5. Piccione, G.; Costa, A.; Fazio, F.; Grasso, F.; Caola, G. Nitrogenous Metabolism in Thoroughbred and Arabian Foals from Birth to Five Months of Age. *Arq. Bras. Med. Vet. Zootec.* **2006**, *58*, 525–529. [CrossRef]
6. Stewart, J.H.; Rose, R.J.; Barko, A.M. Respiratory Studies in Foals from Birth to Seven Days Old. *Equine Vet. J.* **1984**, *16*, 323–328. [CrossRef]
7. Martin-Rosset, W. Growth and Development in the Equine. *Grow. Horse: Nutr. Prev. Growth Disord. EAAP Ser.* **2004**, *114*, 15–50.
8. Ott, E.A. Energy and Protein Metabolism of Normal Growth. *Grow. Horse Nutr. Prev. Growth Disord.* **2005**, *114*, 91.
9. Cymbaluk, N.F. Cold Housing Effects on Growth and Nutrient Demand of Young Horses. *J. Anim. Sci.* **1990**, *68*, 3152–3162. [CrossRef]
10. Cymbaluk, N.F.; Christison, G.I. Environmental Effects on Thermoregulation and Nutrition of Horses. *Vet. Clin. North Am. Equine Pract.* **1990**, *6*, 355–372. [CrossRef]
11. Autio, E.; Heiskanen, M.-L.; Mononen, J. Thermographic Evaluation of the Lower Critical Temperature in Weanling Horses. *J. Appl. Anim. Welf. Sci.* **2007**, *10*, 207–216. [CrossRef]
12. Kronfeld, D.S. Starvation and Malnutrition of Horses: Recognition and Treatment. *J. Equine Vet. Sci.* **1993**, *13*, 298–304. [CrossRef]
13. Whiting, T.L.; Salmon, R.H.; Wruck, G.C. Chronically Starved Horses: Predicting Survival, Economic, and Ethical Considerations. *Can. Vet. J.* **2005**, *46*, 320–324. [PubMed]
14. Mount, L.E. *Adaptation to Thermal Environment. Man and His Productive Animals*; Edward Arnold (Publishers) Ltd.: London, UK, 1979.
15. Curcio, B.R.; Nogueira, C.E.W. Newborn Adaptations and Healthcare throughout the First Age of the Foal. *Anim. Reprod.* **2012**, *9*, 182–187.
16. Autio, E.; Neste, R.; Airaksinen, S.; Heiskanen, M.-L. Measuring the Heat Loss in Horses in Different Seasons by Infrared Thermography. *J. Appl. Anim. Welf. Sci.* **2006**, *9*, 211–221. [CrossRef]
17. McKeever, K.H. Exercise and Rehabilitation of Older Horses. *Vet. Clin. North Am. Equine Pract.* **2016**, *32*, 317–332. [CrossRef]
18. Minkina, W.; Dudzik, S. *Infrared Thermography: Errors and Uncertainties*; John Wiley & Sons: Hoboken, NJ, USA, 2009.
19. Faye, E.; Dangles, O.; Pincebourde, S. Distance Makes the Difference in Thermography for Ecological Studies. *J. Therm. Biol.* **2016**, *56*, 1–9. [CrossRef] [PubMed]
20. Turner, T.A. Diagnostic Thermography. *Vet. Clin. North Am. Equine Pract.* **2001**, *17*, 95–114. [CrossRef]
21. Casas-Alvarado, A.; Mota-Rojas, D.; Hernández-Ávalos, I.; Mora-Medina, P.; Olmos-Hernández, A.; Verduzco-Mendoza, A.; Reyes-Sotelo, B.; Martínez-Burnes, J. Advances in Infrared Thermography: Surgical Aspects, Vascular Changes, and Pain Monitoring in Veterinary Medicine. *J. Therm. Biol.* **2020**, *92*, 102664. [CrossRef]
22. Domino, M.; Borowska, M.; Zdrojkowski, Ł.; Jasiński, T.; Sikorska, U.; Skibniewski, M.; Maśko, M. Application of the Two-Dimensional Entropy Measures in the Infrared Thermography-Based Detection of Rider: Horse Bodyweight Ratio in Horseback Riding. *Sensors* **2022**, *22*, 6052. [CrossRef]
23. Eddy, A.L.; Van Hoogmoed, L.M.; Snyder, J.R. The Role of Thermography in the Management of Equine Lameness. *Vet. J.* **2001**, *162*, 172–181. [CrossRef]
24. Howell, K.; Dudek, K.; Soroko, M. Thermal Camera Performance and Image Analysis Repeatability in Equine Thermography. *Infrared Phys. Technol.* **2020**, *110*, 103447. [CrossRef]
25. Janczarek, I.; Kędzierski, W.; Tkaczyk, E.; Kaczmarek, B.; Łuszczyński, J.; Mucha, K. Thermographic Analysis of the Metacarpal and Metatarsal Areas in Jumping Sport Horses and Leisure Horses in Response to Warm-Up Duration. *Animals* **2021**, *11*, 2022. [CrossRef] [PubMed]

26. Domino, M.; Borowska, M.; Kozłowska, N.; Zdrojkowski, Ł.; Jasiński, T.; Smyth, G.; Maśko, M. Advances in Thermal Image Analysis for the Detection of Pregnancy in Horses Using Infrared Thermography. *Sensors* **2022**, *22*, 191. [CrossRef] [PubMed]
27. Janczarek, I.; Wnuk-Pawlak, E.; Wiśniewska, A.; Dziuban, D.; Frątczak, M.; Raś, B. Body Temperature of Horses Spending Time in Paddocks in Various Weather Conditions during the Summer. *Rocz. Nauk. Pol. Tow. Zootech.* **2020**, *16*, 53–66. [CrossRef]
28. Yarnell, K.; Hall, C.; Royle, C.; Walker, S.L. Domesticated Horses Differ in Their Behavioural and Physiological Responses to Isolated and Group Housing. *Physiol. Behav.* **2015**, *143*, 51–57. [CrossRef]
29. Witkowska-Piłaszewicz, O.; Maśko, M.; Domino, M.; Winnicka, A. Infrared Thermography Correlates with Lactate Concentration in Blood during Race Training in Horses. *Animals* **2020**, *10*, 2072. [CrossRef] [PubMed]
30. Soroko, M.; Howell, K.; Zwyrzykowska, A.; Dudek, K.; Zielińska, P.; Kupczyński, R. Maximum Eye Temperature in the Assessment of Training in Racehorses: Correlations With Salivary Cortisol Concentration, Rectal Temperature, and Heart Rate. *J. Equine Vet. Sci.* **2016**, *45*, 39–45. [CrossRef]
31. Maśko, M.; Witkowska-Piłaszewicz, O.; Jasiński, T.; Domino, M. Thermal Features, Ambient Temperature and Hair Coat Lengths: Limitations of Infrared Imaging in Pregnant Primitive Breed Mares within a Year. *Reprod. Domest. Anim.* **2021**, *56*, 1315–1328. [CrossRef]
32. Stewart, M.; Webster, J.R.; Schaefer, A.L.; Cook, N.J.; Scott, S.L. Infrared Thermography as a Non-Invasive Tool to Study Animal Welfare. *Anim. Welf.* **2005**, *14*, 319–325. [CrossRef]
33. Masko, M.; Borowska, M.; Domino, M.; Jasinski, T.; Zdrojkowski, L.; Gajewski, Z. A Novel Approach to Thermographic Images Analysis of Equine Thoracolumbar Region: The Effect of Effort and Rider's Body Weight on Structural Image Complexity. *BMC Vet. Res.* **2021**, *17*, 99. [CrossRef]
34. Domino, M.; Borowska, M.; Kozłowska, N.; Trojakowska, A.; Zdrojkowski, Ł.; Jasiński, T.; Smyth, G.; Maśko, M. Selection of Image Texture Analysis and Color Model in the Advanced Image Processing of Thermal Images of Horses Following Exercise. *Animals* **2022**, *12*, 444. [CrossRef] [PubMed]
35. Childs, C.; Nwaizu, H.; Voloaca, O.; Shenfield, A. Segmentation Agreement and AI-Based Feature Extraction of Cutaneous Infrared Images of the Obese Abdomen after Caesarean Section: Results from a Single Training Session. *Appl. Sci.* **2023**, *13*, 3992. [CrossRef]
36. Domino, M.; Romaszewski, M.; Jasiński, T.; Maśko, M. Comparison of the Surface Thermal Patterns of Horses and Donkeys in Infrared Thermography Images. *Animals* **2020**, *10*, 2201. [CrossRef]
37. Hodges, M.R.; Tattersall, G.J.; Harris, M.B.; McEvoy, S.D.; Richerson, D.N.; Deneris, E.S.; Johnson, R.L.; Chen, Z.-F.; Richerson, G.B. Defects in Breathing and Thermoregulation in Mice with Near-Complete Absence of Central Serotonin Neurons. *J. Neurosci.* **2008**, *28*, 2495–2505. [CrossRef] [PubMed]
38. Blumberg, M.S.; Deaver, K.; Kirby, R.F. Leptin Disinhibits Nonshivering Thermogenesis in Infants after Maternal Separation. *Am. J. Physiol.-Regul. Integr. Comp. Physiol.* **1999**, *276*, R606–R610. [CrossRef]
39. McKEEVER, K.H.; Eaton, T.L.; Geiser, S.; Kearns, C.F.; Lehnhard, R.A. Age Related Decreases in Thermoregulation and Cardiovascular Function in Horses. *Equine Vet. J.* **2010**, *42*, 220–227. [CrossRef]
40. Preethi, S.; Jhirwal, A.K.; Goswami, S.C.; Legha, R.A.; Kumar, V.; Singh, V. EFFECT OF AMBIENT TEMPERATURE AND RELATIVE HUMIDITY ON THE FOAL'S SKIN SURFACE TEMPERATURE UNDER NORTH AND SOUTH FACING HOUSE IN SEMI-ARID REGIONS. *Vet. Pract.* **2019**, *20*, 135–137.
41. Hampton, C.E. Thermoregulation. In *Manual of Equine Anesthesia and Analgesia*; John Wiley & Sons, Ltd.: Hoboken, NJ, USA, 2022; pp. 173–183. ISBN 978-1-119-63131-6.
42. Sharma, G.; Bala, R. *Digital Color Imaging Handbook*; CRC Press: New York, NY, USA, 2017; ISBN 978-1-351-83597-8.
43. Piccione, G.; Caola, G.; Refinetti, R. Maturation of the Daily Body Temperature Rhythm in Sheep and Horse. *J. Therm. Biol.* **2002**, *27*, 333–336. [CrossRef]
44. Jodkowska, E.; Dudek, K.; Przewozny, M. The Maximum Temperatures (Tmax) Distribution on the Body Surface of Sport Horses. *J. Life Sci.* **2011**, *5*, 291–297.
45. Mejdell, C.M.; Bøe, K.E.; Jørgensen, G.H.M. Caring for the Horse in a Cold Climate—Reviewing Principles for Thermoregulation and Horse Preferences. *Appl. Anim. Behav. Sci.* **2020**, *231*, 105071. [CrossRef]
46. McKenzie, H.C. Disorders of Foals. In *Equine Internal Medicine*; Elsevier: Amsterdam, Netherlands, 2018; pp. 1365–1459, ISBN 978-0-323-44329-6.
47. McManus, C.; Tanure, C.B.; Peripolli, V.; Seixas, L.; Fischer, V.; Gabbi, A.M.; Menegassi, S.R.O.; Stumpf, M.T.; Kolling, G.J.; Dias, E.; et al. Infrared Thermography in Animal Production: An Overview. *Comput. Electron. Agric.* **2016**, *123*, 10–16. [CrossRef]
48. Domino, M.; Borowska, M.; Trojakowska, A.; Kozłowska, N.; Zdrojkowski, Ł.; Jasiński, T.; Smyth, G.; Maśko, M. The Effect of Rider:Horse Bodyweight Ratio on the Superficial Body Temperature of Horse's Thoracolumbar Region Evaluated by Advanced Thermal Image Processing. *Animals* **2022**, *12*, 195. [CrossRef] [PubMed]